INTERNATIONAL JOURNAL FOR NUMERICAL METHODS IN ENGINEERING
Int. J. Numer. Meth. Engng 2011; **87**:171–195
Published online 13 September 2010 in Wiley Online Library (wileyonlinelibrary.com). DOI: 10.1002/nme.3021

Consistent pressure Laplacian stabilization for incompressible continua via higher-order finite calculus

Eugenio Oñate[1,*,†], Sergio R. Idelsohn[1,‡] and Carlos A. Felippa[2,§]

[1]*International Center for Numerical Methods in Engineering* (*CIMNE*), *Technical University of Catalonia* (*UPC*), *Campus Norte UPC*, *08034 Barcelona*, *Spain*
[2]*Department of Aerospace Engineering Sciences and Center for Aerospace Structures*, *University of Colorado*, *Boulder*, *CO 80309-0429*, *U.S.A.*

SUMMARY

We present a stabilized numerical formulation for incompressible continua based on a higher-order Finite Calculus (FIC) approach and the finite element method. The focus of the paper is on the derivation of a stabilized form for the mass balance (incompressibility) equation. The simpler form of the momentum equations neglecting the non-linear convective terms, which is typical for incompressible solids, Stokes flows and Lagrangian flows is used for the sake of clarity. The discretized stabilized mass balance equation adds to the standard divergence of velocity term a pressure Laplacian and an additional boundary term. The boundary term is relevant for the accuracy of the numerical solution, especially for free surface flow problems. The Laplacian and boundary stabilization terms are multiplied by non-linear parameters that have an extremely simple expression in terms of element sizes, the pressure and the discrete residuals of the incompressibility equation and the momentum equations, thus ensuring the consistency of the method. The stabilized formulation allows solving the incompressible problem iteratively using an equal-order interpolation for the velocities (or displacements) and the pressure, which are the only unknowns. The use of additional pressure gradient projection variables, typical of many stabilized methods, is unnecessary.

The formulation is particularly useful for heterogeneous incompressible materials with discontinuous material properties, as it allows computing all the stabilization matrices at the element level. Details of the finite element formulation are given. The good behaviour of the new pressure Laplacian stabilization (PLS) technique is shown in simple but demonstrative examples of application. A very accurate solution was obtained in all cases in 2–3 iterations.

Received 12 February 2010; Revised 13 July 2010; Accepted 14 July 2010

KEY WORDS: pressure Laplacian stabilization; incompressible continua; finite calculus; finite element method

1. INTRODUCTION

It is well known that the finite element solution of incompressible continua requires stabilization in order to obtain physically meaningful solutions.

Stabilization terms are typically needed for two reasons: (1) to avoid spurious velocity oscillations due to large convective terms in the momentum equations of fluid flow problems and (2) to avoid spurious pressure oscillations in incompressible continua when an equal-order interpolation is used for the kinematic variables (the velocities in a fluid or the displacement in a solid) and the pressure [1, 2].

*Correspondence to: Eugenio Oñate, International Center for Numerical Methods in Engineering (CIMNE), Technical University of Catalonia (UPC), Campus Norte UPC, Edificio C1, Gran Capitán s/n, 08034 Barcelona, Spain.
†E-mail: onate@cimne.upc.edu
‡ICREA Research Professor.
§Visiting Professor.

Different stabilization procedures have been proposed over the past three decades. Most methods are based on adding additional terms to the momentum and mass balance (incompressibility) equations. Those terms depend on the residuals of the discrete governing equations [1–35].

In this paper we assume that convective effects are negligible (or even zero) and focuss on the derivation of a new approach to obtain a stabilized equation for the mass balance equation of an incompressible continua using a higher-order finite calculus (FIC) technique [22–26], [30–32] combined with the finite element method (FEM). The discretized stabilized mass balance equation adds to the standard divergence of velocity term a pressure Laplacian and an additional boundary term. The boundary term is relevant for the accuracy of the numerical solution, especially for free surface flow problems. The Laplacian and boundary stabilization terms are multiplied by non-linear parameters that have a simple expression in terms of element sizes, the pressure and the discrete residuals of the incompressibility equation and the momentum equations, thus ensuring the consistency of the method. The stabilized formulation allows solving the incompressible problem iteratively using an equal-order linear interpolation for the velocities (or displacements) and the pressure, which are the only unknowns. The use of additional pressure-gradient projection variables, typical of many stabilized methods, is unnecessary.

It it also shown that the higher-order FIC approach may be used as starting point for deriving a more standard sub-grid-type stabilization method, which uses the pressure gradient projections as additional unknown variables.

The accuracy and efficiency of the new pressure Laplacian stabilization (PLS) procedure are shown in simple but demonstrative examples of application.

2. GOVERNING EQUATIONS

For conciseness we will write the governing equations as usually done in incompressible fluid mechanics [1, 2]. Thus, the equations for an incompressible continuum are expressed in the Lagrangian description using velocity variables as:

Momentum

$$\rho\frac{Dv_i}{Dt}-\frac{\partial\sigma_{ij}}{\partial x_j}-b_i=0 \quad \text{on } \Omega \tag{1}$$

Mass balance (incompressibility)

$$\varepsilon_v:=\frac{\partial v_i}{\partial x_i}=0 \quad \text{on } \Omega, \quad i=1,2,3 \tag{2}$$

In Equations (1) and (2), Ω is the analysis domain, v_i is the velocity along the ith coordinate direction, ρ is the density, σ_{ij} are the Cauchy stresses, b_i are the body forces (typically $b_i=\rho g_i$ where g_i is the component of the gravity along the ith direction) and ε_v is the volumetric strain rate. In addition, in (1) Dv_i/Dt is the total derivative of the velocity. In our work we assume that $Dv_i/Dt=\partial v_i/\partial t$, i.e. convective derivative terms are neglected, as it is usual in Stokes flows and Lagrangian descriptions of incompressible continua [25–29, 33, 34, 36, 37].

The problem is completed with the *boundary conditions* for velocities and tractions, i.e.

$$v_i-v_i^p=0 \quad \text{on } \Gamma_u \tag{3a}$$

$$\sigma_{ij}n_j-t_i^p=0 \quad \text{on } \Gamma_t \tag{3b}$$

where v_i^p denote the prescribed velocities on the Dirichlet boundary Γ_u and t_i^p are the traction forces acting on the Neuman boundary Γ_t, with normal vector $\mathbf{n}=[n_1,n_2,n_3]^{\mathrm{T}}$ (for 3D problems). The total boundary is $\Gamma:=\Gamma_u\cup\Gamma_t$.

In Equations (1)–(3a) and in the following, summation convention for repeated indices in products and derivatives is used unless otherwise specified.

DOI: 10.1002/nme

The Lagrangian governing equations (1)–(3a) hold for incompressible media in both fluid and solid mechanics. The distinction emerges in the constitutive equations, as described next.

Following standard practice, Cauchy stresses are split into deviatoric and pressure components as

$$\sigma_{ij} = s_{ij} + p\delta_{ij} \tag{4}$$

where s_{ij} are the deviatoric stresses, $p = \sigma_{ii}/3$ is the pressure (assumed here to be positive if the mean normal stress is tensile), and δ_{ij} is the Kronećker delta.

For the fluid case we will assume the constitute equations of an isotropic, Newtonian viscous liquid. In that model, deviatoric stresses are related to deformation rates ε_{ij} by

$$s_{ij} = 2\mu(\varepsilon_{ij} - \tfrac{1}{3}\varepsilon_v\delta_{ij}) \tag{5a}$$

where μ is the fluid viscosity and

$$\varepsilon_{ij} = \frac{1}{2}\left(\frac{\partial v_i}{\partial x_j} + \frac{\partial v_j}{\partial x_i}\right), \quad \varepsilon_v := \varepsilon_{ii} \tag{5b}$$

Remark 1

For an *incompressible*, *linear isotropic solid*, the kinematic boundary condition (3a) is usually expressed in terms of displacement variables and the constitutive equation (5a) is written in incremental form [29, 36]. This simplest expression is

$$\Delta s_{ij} = s_{ij}^{n+1} - s_{ij}^{n} = 2G\Delta t[\varepsilon_{ij} - \tfrac{1}{3}\varepsilon_v\delta_{ij}] \tag{6}$$

where Δs_{ij} is the increment of the deviatoric stresses between time steps n and $n+1$, Δt is the time increment and G is the shear modulus. Indeed other incremental forms for the constitutive equation in solids using an objective time derivative of the stresses can be derived [35–37].

3. INTEGRAL FORM OF THE MOMENTUM EQUATIONS

The weighted residual form of Equations (1) and (3b) is

$$\int_\Omega w_i\left[\rho\frac{\partial v_i}{\partial t} - \frac{\partial \sigma_{ij}}{\partial x_j} - b_i\right]\mathrm{d}\Omega + \int_{\Gamma_t} w_i(\sigma_{ij}n_j - t_i^p)\,\mathrm{d}\Gamma = 0 \tag{7}$$

where w_i are the components of an appropriate test function.

Integrating by parts the term involving σ_{ij} in Equation (7) and substituting Equation (4) into the expression for σ_{ij} gives an integral (weak form) expression of the momentum equations as:

$$\int_\Omega\left[w_i\rho\frac{\partial v_i}{\partial t} + \frac{\partial w_i}{\partial x_j}s_{ij} - \frac{\partial w_i}{\partial x_i}p\right]\mathrm{d}\Omega - \int_\Omega w_i b_i\,\mathrm{d}\Omega - \int_{\Gamma_t} w_i t_i^p\,\mathrm{d}\Gamma = 0 \tag{8}$$

Equation (8) is the starting point for the finite element discretization of the momentum equations.

4. ABOUT THE PRESSURE STABILIZATION FOR INCOMPRESSIBLE CONTINUA

Many stabilization procedures for solving incompressible problems in fluid and solid mechanics have been proposed [1–23]. Earlier procedures added to the standard incompressibility equation (either in the strong form or in the variational equation) a pressure Laplacian scaled by a stabilization coefficient that depends on physical parameters and the time step increment. Some of these stabilization methods are described in [1, 2]. A similar stabilization procedure adds to the variational equation a local L_2 polynomial pressure projection multiplied by the inverse of the kinematic viscosity [19]. These approaches are inconsistent since the stabilization term does not vanish for

DOI: 10.1002/nme

the exact solution, which can lead to errors in the pressure distribution and in the preservation of the total volume. An improved approach adds to the incompressibility condition a term that is the function of the discretized momentum equations, thus ensuring consistency. A standard procedure of this kind is the Galerkin least-square (GLS) method [4, 8]. Another procedure of this type, which has attracted much interest recently, is the so-called *pressure-gradient projection stabilization* (PGPS) (also called orthogonal sub-scales stabilization method) [15, 17, 21]. In the PGPS method, pressure gradients are projected onto a continuous field; the difference between the actual gradients and their own projections generates stabilization terms. This is equivalent to replacing the incompressible equation (2) by the following equation:

$$\varepsilon_v + \nabla^{\mathrm{T}}\{\tau(\nabla p + \boldsymbol{\pi})\} = 0 \tag{9}$$

where $\boldsymbol{\pi}$ is a continuous function (termed the pressure gradient projection vector) obtained by projecting the pressure gradient ∇p on the velocity field, and τ is a stabilization parameter. Typically, τ is chosen as a function of the viscosity parameter and the mesh size. The optimal definition of the stabilization parameter is still a challenge in GLS and PGPS methods.

The term $(\nabla p + \boldsymbol{\pi})$ in Equation (9) can be interpreted as the discrete residual of the momentum equations. As a result, the total number of discrete unknown is increased by the inclusion of the $\boldsymbol{\pi}$ field, which is discretized via pressure shape functions. For completeness, the set of governing discrete equations is extended with additional equations requiring the vanishing of the sum $(\nabla p + \boldsymbol{\pi})$ in a weighted residual sense. This ensures the consistency of the method.

PGPS methods are useful for homogeneous flows lacking free-surfaces but encounter severe difficulties for fluids with heterogeneous properties (also called multi-fluids [34, 38]) and, in some cases, for free-surface flows. The two main drawbacks of PGPS methods are:

1. When there are jumps in the physical properties of the fluid, such as the density or the viscosity, the pressure gradient field is discontinuous. The projection of this physical discontinuity on a continuous field introduces large errors in the mass conservation equation.
2. When pressure segregation techniques are used for solving the Navier–Stokes equations, PGPS methods induce errors on the boundary conditions that may lead to unacceptable volume errors. This error is larger for free surface flows [39].

Furthermore, PGPS methods increase the number of problem variables ($\mathbf{u}$, p and $\boldsymbol{\pi}$) as well as the connectivity (bandwidth) of the matrices to be solved. This affects negatively the efficiency of the stabilization procedure and of the overall numerical scheme.

We present herein a procedure, termed PLS for *Pressure Laplacian Stabilization*, that simply adds two stabilization terms to the variational form of the incompressibility equation: (1) a pressure Laplacian and (2) a boundary integral. Both terms are multiplied by residual-dependent stabilization parameters which expression emerges naturally from the formulation. Consistency is preserved since the stabilization parameters vanish for the exact solution. An advantage of the new stabilization terms is that the Laplace matrix and the boundary matrix are computed at element level. Accordingly, the connectivity (bandwidth) of the unstabilized matrices is not affected. Because pressure gradient continuity is not enforced, as it happens in PGPS methods, the treatment of heterogeneous multi-fluid problems, such as mixing, is facilitated.

A serendipitous advantage is that the inclusion of the boundary term sidesteps the need for prescribing known boundary pressure values when a segregated solution procedure is used. This is essential for ensuring the overall conservation of mass in the analysis domain for free surface flows [39].

An apparent drawback of the PLS method is that the resulting stabilized equation is non-linear (due to the residual dependence of the stabilization parameters) and this requires using an iterative solution scheme. Convergence of the solution has been found, however, in 2–3 iterations for all the problems tested in this work. In addition, the non-linearity can be easily handled within a time-integration scheme in transient problems, or in practical problems where other non-linearities might appear due to the presence of convective terms in the momentum equations (such as in Navier–Stokes flows) or non-linear material behaviour.

DOI: 10.1002/nme

5. STABILIZED FORM OF THE MASS BALANCE EQUATION VIA HIGHER-ORDER FINITE CALCULUS

5.1. On the proportionality of the pressure and the volumetric strain rate

Let us assume a relationship between the pressure and the volumetric strain rate typical for 'compressible' and 'quasi-incompressible' materials, as

$$\frac{1}{K}p=\varepsilon_v \tag{10}$$

where K is the bulk modulus. Clearly for a full incompressible material $K=\infty$ and $\varepsilon_v=0$. For finite, although very large, values of K the following expression can be readily deduced from Equation (10):

$$\frac{1}{K}\nabla p=\nabla\varepsilon_v \tag{11}$$

where ∇ is the gradient operator. For 2D problems, $\nabla=[\partial/\partial x_1, \partial/\partial x_2]^{\mathrm{T}}$.

Equation (11) shows that pressure and volumetric strain rate gradients are co-directional for any $K\neq 0$. We will assume that this property also holds for the full incompressible case (at least for values of K comfortably representable on the computer without overflow). From Equations (10) and (11) we deduce

$$\frac{\nabla\varepsilon_v}{|\nabla\varepsilon_v|}=\frac{\nabla p}{|\nabla p|} \quad \text{and hence} \quad \frac{\partial\varepsilon_v}{\partial x_i}=\frac{\partial p}{\partial x_i}\frac{|\nabla\varepsilon_v|}{|\nabla p|} \tag{12}$$

5.2. Higher-order FIC form of the mass balance equation

The Finite Calculus (FIC) form of the mass balance equation for the full incompressible case is obtained by using a higher-order Taylor series expansion for expressing the balance of mass in a finite size domain in terms of values of the velocity derivatives at the center of the domain (Figure A1 of Appendix A). The higher-order FIC mass balance equation is written for 2D problems as:

$$\varepsilon_v+\frac{h_1^2}{24}\frac{\partial^2\varepsilon_v}{\partial x_1^2}+\frac{h_2^2}{24}\frac{\partial^2\varepsilon_v}{\partial x_2^2}=0 \tag{13}$$

In Equation (13) h_1 and h_2 are the sizes of the rectangular domain where the mass balance is enforced. The derivation of Equation (13) is shown in Appendix A. Clearly for the infinitesimal case $h_1=h_2=0$ and the standard incompressibility equation ($\varepsilon_v=0$) is recovered.

Equation (13) can be interpreted as a *non-local* mass balance equation incorporating the size of the domain used to enforce the mass balance condition and higher-order second derivative terms of the volumetric strain rate. Equation (13) can be extended to account for temporal stabilization terms. These terms, however, are disregarded here as they have not be found to be relevant for the problems investigated so far.

Remark 2

In previous works we have developed stabilized FIC form of the mass balance equation obtained by expressing the velocity derivatives in terms of their values sampled at the corner points of the mass balance domain via Taylor series and retaining the second derivatives of the velocities only. The resulting expression is [22–26].

$$\varepsilon_v\pm\tfrac{1}{2}\mathbf{h}^{\mathrm{T}}\nabla\varepsilon_v=0 \tag{14}$$

For 2D problems $\mathbf{h}=[h_1, h_2]^{\mathrm{T}}$. The sign in Equation (14) is positive or negative depending whether the sampling point at which velocity derivatives are computed is the corner node 1 or 7

DOI: 10.1002/nme

in Figure A1, respectively. The sign in Equation (14) is irrelevant in practice. Equation (14) will be used for deriving the expression for the stabilization parameters in Section 5.4.

5.3. Weighted residual form of the higher-order FIC mass balance equation

The weighted residual form of Equation (13) is

$$\int_\Omega q\left(\varepsilon_v+\frac{h_1^2}{24}\frac{\partial^2\varepsilon_v}{\partial x_1^2}+\frac{h_2^2}{24}\frac{\partial^2\varepsilon_v}{\partial x_2^2}\right)\mathrm{d}\Omega=0 \tag{15}$$

where q are adequate test functions.

Integrating by parts the second derivative terms in Equation (15) gives

$$\int_\Omega q\varepsilon_v\,\mathrm{d}\Omega-\int_\Omega\left(\frac{h_1^2}{24}\frac{\partial q}{\partial x_1}\frac{\partial\varepsilon_v}{\partial x_1}+\frac{h_2^2}{24}\frac{\partial q}{\partial x_2}\frac{\partial\varepsilon_v}{\partial x_2}\right)\mathrm{d}\Omega+\int_\Gamma\frac{q}{24}\left(n_1h_1^2\frac{\partial\varepsilon_v}{\partial x_1}+n_2h_2^2\frac{\partial\varepsilon_v}{\partial x_2}\right)\mathrm{d}\Gamma=0 \tag{16}$$

where n_i are the components of the normal vector to the boundary Γ.

In the derivation of Equation (16), space derivatives of the characteristic lengths h_1 and h_2 have been neglected. This assumption holds exactly if both lengths are taken to be constant over the rectangular domain (or locally constant at each integration point). In any case this assumption does not invalidate the derivation, as long as the discretized formulation converges to correct velocity and pressure fields satisfying the momentum and incompressibility equations in an average sense and up to the desired order of accuracy.

Using the relationships in Equation (12) we can write

$$\begin{aligned}\int_\Omega\left(\frac{h_1^2}{24}\frac{\partial q}{\partial x_1}\frac{\partial\varepsilon_v}{\partial x_1}+\frac{h_2^2}{24}\frac{\partial q}{\partial x_2}\frac{\partial\varepsilon_v}{\partial x_2}\right)\mathrm{d}\Omega&=\int_\Omega\left(h_1^2\frac{\partial q}{\partial x_1}\frac{\partial p}{\partial x_1}+h_2^2\frac{\partial q}{\partial x_2}\frac{\partial p}{\partial x_2}\right)\frac{|\nabla\varepsilon_v|}{24|\nabla p|}\,\mathrm{d}\Omega\\&=\int_\Omega\left(\sum_{i=1}^{2}\tau_i\frac{\partial q}{\partial x_i}\frac{\partial p}{\partial x_i}\right)\mathrm{d}\Omega\end{aligned} \tag{17}$$

with

$$\tau_i=\frac{h_i^2|\nabla\varepsilon_v|}{24|\nabla p|},\quad i=1,2\quad\text{(for 2D problems)} \tag{18}$$

Substituting Equations (17) and (20) into (16) we write the stabilized mass balance equation as:

$$\boxed{\int_\Omega q\varepsilon_v\,\mathrm{d}\Omega-\int_\Omega(\nabla^{\mathrm{T}}q)\mathbf{D}_v\nabla p\,\mathrm{d}\Omega+\int_\Gamma qg\,\mathrm{d}\Gamma=0} \tag{19}$$

For 2D problems

$$\mathbf{D}_v=\begin{bmatrix}\tau_1 & 0\\ 0 & \tau_2\end{bmatrix}\quad\text{and}\quad g=\sum_{i=1}^{2}\frac{h_i^2}{24}n_i\frac{\partial\varepsilon_v}{\partial x_i} \tag{20}$$

5.4. Computation of the domain stabilization parameters τ_i

The momentum equations (1) can be written using Equations (4) and (5a) as:

$$\rho\frac{\partial v_i}{\partial t}-\frac{\partial}{\partial x_j}(2\mu\varepsilon_{ij})+\frac{2}{3}\mu\frac{\partial\varepsilon_v}{\partial x_i}-\frac{\partial p}{\partial x_i}-b_i=0 \tag{21}$$

DOI: 10.1002/nme

From Equation (21) we deduce (neglecting space variations of the viscosity)

$$\frac{2}{3}\mu\frac{\partial\varepsilon_v}{\partial x_i}=r_{m_i} \tag{22}$$

with

$$r_{m_i}:=-\rho\frac{\partial v_i}{\partial t}+\frac{\partial}{\partial x_j}(2\mu\varepsilon_{ij})+\frac{\partial p}{\partial x_i}+b_i \tag{23}$$

and, hence

$$\tfrac{2}{3}\mu|\nabla\varepsilon_v|=|\mathbf{r}_m| \tag{24}$$

where $\mathbf{r}_m=[r_{m_1},r_{m_2}]^{\mathrm{T}}$ is the vector containing the momentum equations.

From the first-order FIC mass balance equation (14) (with the negative sign) we deduce

$$\tfrac{1}{2}h_\xi|\nabla\varepsilon_v|=\varepsilon_v \tag{25}$$

where h_ξ is the projection of $\mathbf{h}$ along the gradient of ε_v, i.e.

$$h_\xi=\frac{h_i}{|\nabla\varepsilon_v|}\frac{\partial\varepsilon_v}{\partial x_i}=\frac{\mathbf{h}^{\mathrm{T}}\nabla\varepsilon_v}{|\nabla\varepsilon_v|} \tag{26}$$

Equations (24) and (25) are consistently modified as follows:

$$\tfrac{2}{3}\mu|\mathbf{v}||\nabla\varepsilon_v|=|\mathbf{v}||\mathbf{r}_m| \tag{27}$$

$$\tfrac{1}{2}ph_\xi|\nabla\varepsilon_v|=p\varepsilon_v \tag{28}$$

In Equation (27) $\mathbf{v}$ is the modulus of the velocity vector.

For the discretized problem the r.h.s. of Equations (27) and (28) represents the power of the residual forces in the momentum equations and of the volumetric strain rate, respectively. Clearly, these powers will vanish for the exact solution. Note also that the product ph_ξ in Equation (28) is always positive, as $p\varepsilon_v\geqslant 0$.

From Equations (27) and (28) we deduce

$$|\nabla\varepsilon_v|=\frac{p\varepsilon_v+|\mathbf{v}||\mathbf{r}_m|}{\frac{1}{2}|ph_\xi|+\frac{2}{3}\mu|\mathbf{v}|} \tag{29}$$

Substituting Equation (29) into (18) gives the expression for the stabilization parameters as:

$$\boxed{\tau_i=\frac{h_i^2(p\varepsilon_v+|\mathbf{v}||\mathbf{r}_m|}{(12|ph_\xi|+16\mu|\mathbf{v}|)|\nabla p|}} \tag{30}$$

Note that the expression of τ_i in Equation (30) will vanish for values of v_i and p satisfying *exactly* the incompressibility equation ($\varepsilon_v=0$) and the momentum equations ($|\mathbf{r}_m|=0$). Clearly for the discrete problem, the stabilization parameters depend on the numerical errors in the approximation for ε_v and $\mathbf{r}_m$, as it is desirable. In practice, it is advisable to choose a cut-off value for τ_i. In our work we have chosen the following limiting band: $10^{-8}\leqslant\tau_i\leqslant 10^5$.

DOI: 10.1002/nme

Remark 3
Using only Equation (25) for defining $|\nabla\varepsilon_v|$ and substituting this into Equation (18) gives

$$\tau_i = \frac{h_i^2 |\mathbf{r}_m|}{16\mu |\nabla p|} \tag{31}$$

In the absence of body forces and assuming steady-state conditions and a linear FE approximation, then $|\mathbf{r}_m| = |\nabla p|$ and

$$\tau_i = \frac{h_i^2}{16\mu} \tag{32}$$

which is a form of the stabilization parameter typically found in the literature for Stokes flow [1, 2, 17, 22, 25].

Remark 4
Other residual-based expressions for the stabilization parameter τ_i can be found. For instance, two alternative expressions for τ_i are

$$\tau_i = \frac{h_i^2}{|\nabla p|} \frac{\left(\rho|\mathbf{v}| + \dfrac{\rho|h_\xi|}{2\Delta t}\right)|\varepsilon_v| + |\mathbf{r}_m|}{\left(12\rho|h_\xi \mathbf{v}| + 6\rho\dfrac{h_\xi^2}{\Delta t} + 16\mu\right)} \tag{33}$$

and

$$\tau_i = h_i^2 \left[\frac{\rho|h_\xi \mathbf{v}| + \mu}{24\rho|h_\xi \mathbf{v}|\left|\frac{p}{\varepsilon_v}\right| + 16\mu^2 \dfrac{|\nabla p|}{|\mathbf{r}_m|}} \right] \tag{34}$$

The derivation of above expressions is shown in Appendix B. The merits and drawbacks of the different expressions for τ_i will be studied in a subsequent work [40].

5.5. PLS boundary stabilization term

For the computation of the boundary integral in Equation (19) we proceed as follows.

From the relationships in Equation (12) we express the boundary term g of Equation (20) as

$$g = \sum_{i=1}^{2} \frac{h_i^2}{24} n_i \frac{\partial \varepsilon_v}{\partial x_i} = \sum_{i=1}^{2} \frac{h_i^2}{24} n_i \frac{|\nabla\varepsilon_v|}{|\nabla p|} \frac{\partial p}{\partial x_i} = \tau_{b_i} \frac{\partial p}{\partial x_i} \tag{35a}$$

where τ_{b_i} is a boundary stabilization parameter given by

$$\tau_{b_i} = \frac{h_i^2 n_i |\nabla\varepsilon_v|}{24|\nabla p|} \quad \text{no sum in } i \tag{35b}$$

Substituting the expression for $|\nabla\varepsilon_v|$ of Equation (29) into (34) we find

$$\boxed{\tau_{b_i} = \tau_i n_i} \quad \text{no sum in } i \tag{35c}$$

where τ_i is given by Equation (30) (or by Equations (33) or (34)) with all the terms computed at the boundary edge.

The boundary integral in Equation (19) is finally expressed in terms of the pressure gradient components as:

$$\int_\Gamma q \tau_{b_i} \frac{\partial p}{\partial x_i} \, \mathrm{d}\Gamma \tag{36}$$

DOI: 10.1002/nme

Remark 5
For $h_i = h_j = h$ then $\tau_i = \tau$ and $\tau_{b_i} = \tau n_i$. In this case, the boundary integral (36) can be expressed as

$$\int_\Gamma q\tau \frac{\partial p}{\partial n} \mathrm{d}\Gamma \tag{37}$$

where $\partial p/\partial n = n_i \partial p/\partial x_i$ is the gradient of the pressure normal to the boundary.

5.6. PLS characteristic lengths

The definition of the characteristic distances h_i is a relatively minor issue given the consistency of the expressions for the stabilization parameters (they vanish for the exact solution). Any expression relating the h_i distances to the element sizes can be used in practice.

In our work we have used the following definition for h_i:

$$h_i = \max[\mathbf{l}_j^{\mathrm{T}} \mathbf{a}_j], \quad j = 1, n_s \tag{38}$$

with $\mathbf{a}_1 = [1, 0]^{\mathrm{T}}$ and $\mathbf{a}_2 = [0, 1]^{\mathrm{T}}$ for 2D problems, $\mathbf{l}_i$ are the vectors along the sides of the element and n_s is the number of sides ($n_s = 3$ for triangles). For instance, for side 1 of a triangle linking nodes 2 and 3, $\mathbf{l}_i = [x_1^3 - x_1^2, x_2^3 - x_2^2]^{\mathrm{T}}$, where x_1^i, x_2^i are the horizontal and vertical coordinates of node i.

For the examples solved in this paper results using the expression for h_i of Equation (38) have been found to be very similar to those using a constant value for h_i defined as:

$$h_i = h^e \quad \text{with } h^e = [A^e]^{1/2} \tag{39}$$

6. FINITE ELEMENT DISCRETIZATION

We will discretize the domain Ω with a mesh of standard three-noded triangles (for 2D) or four-noded tetrahedra (for 3D).

The velocities and the pressure are interpolated over each element using the same linear approximation as (for 3D problems)

$$\mathbf{v} = \begin{Bmatrix} v_1 \\ v_2 \\ v_3 \end{Bmatrix} = \sum_{i=1}^{n} \mathbf{N}_i \bar{\mathbf{v}}_i, \quad p = \sum_{i=1}^{n} N_i \bar{p}_i \tag{40}$$

where $\mathbf{N}_i = N_i \mathbf{I}_d$, N_i is the standard linear shape function for node i, $\mathbf{I}_d$ is the $d \times d$ unit matrix, d is the number of space dimensions, n is the number of nodes in the element ($n = 3/4$ for linear triangles/tetrahedra) and $\bar{\mathbf{v}}_i$ and $\bar{p}_i$ are the nodal values of the velocity vector components and the pressure, respectively. Indeed, any other approximation for $\mathbf{v}$ and p can be used.

Substituting the approximation (40) into the governing equations (8) and (19) and choosing $w_i = N_i$ gives the following global system of equations:

$$\begin{bmatrix} \mathbf{M} & \mathbf{0} \\ \mathbf{0} & \mathbf{0} \end{bmatrix} \frac{\mathrm{d}}{\mathrm{d}t} \begin{Bmatrix} \bar{\mathbf{v}} \\ \bar{\mathbf{p}} \end{Bmatrix} + \begin{bmatrix} \mathbf{K} & \mathbf{Q} \\ \mathbf{Q}^{\mathrm{T}} & -(\mathbf{L} - \mathbf{B}) \end{bmatrix} \begin{Bmatrix} \bar{\mathbf{v}} \\ \bar{\mathbf{p}} \end{Bmatrix} = \begin{Bmatrix} \mathbf{f} \\ \mathbf{0} \end{Bmatrix} \tag{41}$$

DOI: 10.1002/nme

The matrices and vectors in Equation (41) are formed by assembling the element contributions given in Box 1 for 3D problems.

$$\mathbf{M}^e_{ij}=\int_{\Omega^e}\rho\mathbf{N}_i^{\mathrm{T}}\mathbf{N}_j\,\mathrm{d}\Omega,\quad \mathbf{K}^e_{ij}=\int_{\Omega^e}\mathbf{G}_i^{\mathrm{T}}\mathbf{D}\mathbf{G}_j\,\mathrm{d}\Omega,\quad \mathbf{Q}^e_{ij}=\int_{\Omega^e}\mathbf{G}_i^{\mathrm{T}}\mathbf{m}N_j\,\mathrm{d}\Omega$$

with

$$\mathbf{G}_i=\begin{bmatrix}\dfrac{\partial N_i}{\partial x_1} & 0 & 0\\ 0 & \dfrac{\partial N_i}{\partial x_2} & 0\\ 0 & 0 & \dfrac{\partial N_i}{\partial x_3}\\ \dfrac{\partial N_i}{\partial x_2} & \dfrac{\partial N_i}{\partial x_1} & 0\\ \dfrac{\partial N_i}{\partial x_3} & 0 & \dfrac{\partial N_i}{\partial x_1}\\ 0 & \dfrac{\partial N_i}{\partial x_3} & \dfrac{\partial N_i}{\partial x_2}\end{bmatrix},\quad \mathbf{m}=[1,1,1,0,0,0]^{\mathrm{T}},\quad \mathbf{D}=\mu\begin{bmatrix}2\mathbf{I}_3 & 0\\ 0 & \mathbf{I}_3\end{bmatrix}$$

$$L^e_{ij}=\int_{\Omega^e}\tau_k\frac{\partial N_i}{\partial x_k}\frac{\partial N_j}{\partial x_k}\,\mathrm{d}\Omega,\quad B^e_{ij}=\int_{\Gamma}\tau_{b_k}N_i\frac{\partial N_j}{\partial x_k}\,\mathrm{d}\Gamma$$

$$\mathbf{f}^e_i=\int_{\Omega^e}N_i\mathbf{b}\,\mathrm{d}\Omega+\int_{\Gamma^e_t}N_i\mathbf{t}^p\,\mathrm{d}\Gamma,\quad i,j=1,2,3$$

$\mathbf{I}_3:3\times 3$unit matrix, $\mathbf{b}=[b_1,b_2,b_3]^{\mathrm{T}}$, $\mathbf{t}^p=[t^p_1,t^p_2,t^p_3]^{\mathrm{T}}$
Γ^e_t: boundary of element e coincident with the external Neuman boundary

Box 1. Element expression of the matrices and vectors in Equation (41) for 3D problems.

Matrix **M** is computed with a three point Gauss quadrature. The rest of the matrices and vectors in Equation (41) are computed with only a one-point quadrature. A higher-order quadrature might be required in some cases for integrating the non-linear terms in matrices **L** and **B**. The simple one-point quadrature has however sufficient to obtain good results for the problems solved in the paper.

A monolithic transient solution of the system of Equations (41) can be found using the following iterative scheme:

$${}^{j+1}\begin{Bmatrix}\bar{\mathbf{v}}\\ \bar{\mathbf{p}}\end{Bmatrix}^{n+1}=[{}^{j}\mathbf{H}^{n+1}]^{-1}\begin{Bmatrix}\mathbf{f}+\dfrac{1}{\Delta t}\mathbf{M}\bar{\mathbf{v}}^n\\ \mathbf{0}\end{Bmatrix}\tag{42a}$$

with

$$\mathbf{H}=\begin{bmatrix}\mathbf{K}+\dfrac{1}{\Delta t}\mathbf{M} & \mathbf{Q}\\ \mathbf{Q}^{\mathrm{T}} & -(\mathbf{L}-\mathbf{B})\end{bmatrix}\tag{42b}$$

DOI: 10.1002/nme

In Equations (42b) $(\cdot)^n$ and $(\cdot)^{n+1}$ denote values at times t and $t+\Delta t$, respectively, whereas the upper left index j denotes the iteration number; i.e. ${}^j(\cdot)^{n+1}$ denotes values at time $t+\Delta t$ and the jth iteration.

For the steady-state case, we can solve for the velocity and pressure variables simultaneously by inverting the system

$$\mathbf{H}_s\mathbf{a}=\bar{\mathbf{f}} \tag{43a}$$

with

$$\mathbf{a}=\begin{Bmatrix}\bar{\mathbf{v}}\\ \bar{\mathbf{p}}\end{Bmatrix},\quad \mathbf{H}_s=\begin{bmatrix}\mathbf{K} & \mathbf{Q}\\ \mathbf{Q}^{\mathrm{T}} & -(\mathbf{L}-\mathbf{B})\end{bmatrix},\quad \bar{\mathbf{f}}=\begin{Bmatrix}\mathbf{f}\\ \mathbf{0}\end{Bmatrix} \tag{43b}$$

Clearly, as the stabilization parameters are a function of the velocity and the pressure, the solution of Equation (43a) must be found iteratively. A simple direct iteration scheme gives

$${}^{j+1}\mathbf{a}=[{}^j\mathbf{H}_s]^{-1}\mathbf{f} \tag{44}$$

where, as usual, j denotes the iteration number.

For transient problems, an *implicit segregated approach* has typically more advantages. For instant, the following iterative scheme can be used for computing $\bar{\mathbf{v}}$ and $\bar{\mathbf{p}}$ in time as

Step 1

$${}^{j+1}\bar{\mathbf{v}}^{n+1}=\bar{\mathbf{v}}^n+\left[\frac{1}{\Delta t}\mathbf{M}+\mathbf{K}\right]^{-1}[\mathbf{f}+\mathbf{Q}^j\bar{\mathbf{p}}^{n+1}] \tag{45a}$$

Step 2

$${}^{j+1}\bar{\mathbf{p}}^{n+1}=[{}^j\mathbf{L}^{n+1}-{}^j\bar{\mathbf{B}}^{n+1}]^{-1}[\mathbf{Q}^{\mathrm{T}\,j+1}\bar{\mathbf{v}}^{n+1}] \tag{45b}$$

Neglecting matrix $\mathbf{B}$ in Equation (47) would require prescribing the pressure at some point of the domain for inverting the Laplace matrix $\mathbf{L}$. As mentioned earlier, the typical option of making $p=0$ at a free boundary introduces an error in the mass conservation equation leading to *considerable mass losses* for viscous free surface flow problems [39]. The presence of the boundary mass matrix $\mathbf{B}$ in Equation (45b) avoids the need for prescribing the pressure at the boundary and this is another distinct feature of the PLS formulation.

Remark 6

The boundary matrix $\mathbf{B}$ is non-symmetrical. Symmetry of the system matrix $\mathbf{H}_s$ can be recovered by shifting the boundary terms to the r.h.s. of Equation (43a). This gives

$$\mathbf{H}_s=\begin{bmatrix}\mathbf{K} & \mathbf{Q}\\ \mathbf{Q}^{\mathrm{T}} & -\mathbf{L}\end{bmatrix},\quad \bar{\mathbf{f}}=\begin{Bmatrix}\mathbf{f}\\ \mathbf{f}_p\end{Bmatrix} \tag{46a}$$

with

$$f_{p_i}=\int_\Gamma N_i\tau_{b_k}\frac{\partial p}{\partial x_k}\,\mathrm{d}\Gamma \tag{46b}$$

The boundary force vector $\mathbf{f}_p$ is now computed at each iteration as part of the iterative process. For the examples solved in the paper we have found that this does not increase the total number of iterations.

Remark 7

Symmetry of the boundary stabilization matrix can also be recovered by defining matrix $\mathbf{B}$ as:

$$B^e_{ij}=\int_\Gamma \bar{\tau}_{b_i}N_iN_j\,\mathrm{d}\Gamma\quad\text{with }\bar{\tau}_b=\frac{\tau_{b_k}}{p}\frac{\partial p}{\partial x_k} \tag{47}$$

DOI: 10.1002/nme

Matrix B_{ij}^e of Equation (47) has now the form of a boundary mass-type matrix. The price for the symmetry of **B** is the increased non-linearity of the boundary stabilization parameter. The usefulness of this alternative will be investigated in the future research.

7. PRESSURE-GRADIENT PROJECTION FORMULATION

An alternative stabilized formulation can be derived from the higher-order FIC equations by introducing the so-called *pressure-gradient projection* variables. The resulting stabilized mass balance equations can be derived in a number of ways [1, 2, 15–18, 20, 21, 29–33]. Here we show how a PGPS (for pressure-gradient projection stabilization) formulation can be readily obtained following the higher-order FIC approach previously described.

From the momentum equations it can be found

$$\frac{h_i^2}{24}\frac{\partial \varepsilon_v}{\partial x_i} = \hat{\tau}_i r_{m_i} \tag{48}$$

where r_{m_i} is defined in Equation (23). The stabilization parameter $\hat{\tau}_i$ is [20, 21, 23]

$$\hat{\tau}_i = \frac{h_i^2}{24}\left[\frac{\rho l^2}{4\Delta t} + \frac{2\mu}{3}\right]^{-1} \tag{49}$$

and l is a typical grid distance. The expression for $\hat{\tau}_i$ of Equation (49) can be also obtained as a particular case of Equation (33).

The FIC characteristic lengths h_i are expressed in terms of the grid distance l as

$$h_i = \alpha_i l \tag{50}$$

where α_i is a numerical parameter.

Introducing Equation (50) into (49) the stabilization parameter for the PGPS method is obtained as:

$$\hat{\tau}_i = \frac{\alpha_i^2}{\left[\dfrac{6\rho}{\Delta t} + 16\dfrac{\mu}{l^2}\right]} \tag{51}$$

Note that Equation (51) is applicable for the viscous (Stokes) and inviscid limit cases.

For relatively fine grids, the numerical solution is insensitive to the values of α_i [25]. For the coarse mesh used in the examples of Section 9 we have obtained good results for the range of values of α_i such that $\sqrt{2} \leqslant \alpha_i \leqslant \sqrt{6}$. More specifically for the computations shown in the paper we have chosen $\alpha_i = \alpha = \sqrt{6}$ and, hence

$$\hat{\tau}_i = \hat{\tau} = \frac{1}{\left[\dfrac{\rho}{\Delta t} + \dfrac{8\mu}{3l^2}\right]} \tag{52}$$

As for the element distance l we have taken $l = 2[\Omega^e]^{1/2}$ for three-noded triangular meshes.

The value of $\hat{\tau}$ in Equation (52) coincides with that deduced in previous works using other arguments [23, 25, 26].

Equations (51) and (52) show that the stabilization parameters in the PGPS method are constant for each element. This is an important difference versus the PLS formulation where a non-linear (and consistent) form for the stabilization parameters is used.

The momentum residuals r_{m_i} are now split as follows:

$$r_{m_i} := \frac{\partial p}{\partial x_i} + \frac{1}{\hat{\tau}_i}\pi_i \quad \text{(no sum in } i\text{)} \tag{53a}$$

DOI: 10.1002/nme

with

$$\pi_i = \hat{\tau}_i \left(-\rho \frac{\partial v_i}{\partial t} + \frac{\partial s_{ij}}{\partial x_j} + b_i \right) \tag{53b}$$

is the ith pressure-gradient projection weighted by the ith stabilization parameter. Note that the sum $(\partial p/\partial x_i) + 1/\hat{\tau}_i \pi_i$ vanishes for the exact solution for which $r_{m_i} = 0$. The π_i's are now taken as additional variables which are discretized with the standard FEM in the same manner as for the pressure.

The form of r_{m_i} in Equation (53a) has been chosen so as to ensure that the term $(1/\hat{\tau}_i)\pi_i$ is discontinuous between adjacent elements after discretization. This is essential for accurately capturing high discontinuous pressure gradient jumps typical of fluids with heterogeneous physical properties (either the viscosity or the pressure) [34, 38, 41]. In this manner the term $\frac{1}{\hat{\tau}_i}\pi_i$ can match the discrete pressure gradient term $\partial p/\partial x_i$, which is naturally discontinuous between elements for a linear approximation of the pressure.

Remark 8

The form of π_i in Equation (53b) is motivated by the recent work of the first two authors on modelling of multi-fluids with different physical properties [34, 41]. A slightly different expression for π_i was chosen in [34, 41] as

$$\pi_i = \frac{1}{\rho}\left[-\rho \frac{\partial v_i}{\partial t} + \frac{\partial s_{ij}}{\partial x_i} + b_i \right] \quad \text{and hence} \quad r_{m_i} := \frac{\partial p}{\partial x_i} + \rho \pi_i \tag{54}$$

The form of π_i of Equation (53b) chosen here leads to similar good results for the pressure gradient jumps (Section 9.2) and has been found to be simpler to implement in practice.

Substituting Equation (48) into the second and third integral of Equation (16) and using (53a) give (for 2D problems)

$$\int_\Omega q \varepsilon_v \, \mathrm{d}\Omega - \int_\Omega \sum_{i=1}^{2} \frac{\partial q}{\partial x_i} \left(\hat{\tau}_i \frac{\partial p}{\partial x_i} + \pi_i \right) \mathrm{d}\Omega + \int_\Gamma q \sum_{i=1}^{2} n_i \left(\hat{\tau}_i \frac{\partial p}{\partial x_i} + \pi_i \right) \mathrm{d}\Gamma = 0 \tag{55}$$

The boundary integral in Equation (55) is typically neglected in PGPS formulations and will be disregarded from here onward.

The following addition equation is introduced for computing the pressure gradient projection variables π_i

$$\int_\Omega \sum_{i=1}^{2} \bar{w}_i \left(\frac{\partial p}{\partial x_i} + \frac{1}{\hat{\tau}_i} \pi_i \right) \mathrm{d}\Omega = 0 \tag{56}$$

In our work $\bar{w}_i = q = N_i$ is chosen.

Clearly, the term $(\partial p/\partial x_i) + (1/\hat{\tau}_i)\pi_i$ (no sum in i) vanishes for the exact solution (see Equation (53a)) and this ensures the consistency of the method.

The next step is the space discretization of the velocities v_i, the pressure p and the pressure-gradient projections π_i in terms of nodal values. In our work a standard linear interpolation is used for all variables. The resulting system of discretized equations is

$$\mathbf{M}\dot{\bar{\mathbf{v}}} + \mathbf{K}\bar{\mathbf{v}} + \mathbf{Q}\bar{\mathbf{p}} = \mathbf{f} \tag{57a}$$

$$\mathbf{Q}\bar{\mathbf{v}} - \mathbf{L}\bar{\mathbf{p}} - \mathbf{C}\bar{\boldsymbol{\pi}} = \mathbf{0} \tag{57b}$$

$$\mathbf{T}\bar{\boldsymbol{\pi}} + \mathbf{C}^{\mathrm{T}}\bar{\mathbf{p}} = 0 \tag{57c}$$

DOI: 10.1002/nme

where all matrices and vectors are defined in Box 1 except $\mathbf{T}$ and $\mathbf{C}$ given (for each element) by

$$\mathbf{T}^e = \begin{bmatrix} \hat{\mathbf{T}}_1^e & \mathbf{0} & \mathbf{0} \\ \mathbf{0} & \hat{\mathbf{T}}_2^e & \mathbf{0} \\ \mathbf{0} & \mathbf{0} & \hat{\mathbf{T}}_3^e \end{bmatrix}, \quad [\hat{T}_i^e]_{kl} = \int_{\Omega^e} \frac{1}{\hat{\tau}_i} N_k N_l \, \mathrm{d}\Omega, \quad k,l = 1,2,3$$
$$\mathbf{C}^e = [\mathbf{Q}^e, \mathbf{Q}^e, \mathbf{Q}^e] \tag{58}$$

In Equations (57) $\bar{(\cdot)}$ as usual denotes nodal values for the corresponding variables and $\dot{\bar{\mathbf{v}}} = \partial \bar{\mathbf{v}}/\partial t$. As mentioned earlier in the derivation of Equation (57b) we have disregarded the contribution of the boundary term in Equation (55). The solution of Equations (57a) is typically performed via an iterative staggered scheme.

The nodal pressure-gradient projection values $\bar{\boldsymbol{\pi}}$ can be eliminated from Equation (57c) using a diagonal form for $\mathbf{T}$ as:

$$\bar{\boldsymbol{\pi}} = -\mathbf{T}_d^{-1}\mathbf{C}^{\mathrm{T}}\bar{\mathbf{p}} \quad \text{where } \mathbf{T}_d = \mathrm{diag}(\mathbf{T}) \tag{59}$$

Substituting $\bar{\boldsymbol{\pi}}$ from Equation (59) into (57b) yields the following system of two equations for $\bar{\mathbf{v}}$ and $\bar{\mathbf{p}}$:

$$\mathbf{M}\dot{\bar{\mathbf{v}}} + \mathbf{K}\bar{\mathbf{v}} + \mathbf{Q}\bar{\mathbf{p}} = \mathbf{f} \tag{60a}$$

$$\mathbf{Q}\bar{\mathbf{v}} - (\mathbf{L} - \hat{\mathbf{L}})\bar{\mathbf{p}} = \mathbf{0} \tag{60b}$$

where $\hat{\mathbf{L}} = \mathbf{C}\mathbf{T}_d^{-1}\mathbf{C}^{\mathrm{T}}$ is the *discrete pressure Laplace matrix*. This matrix has a wider bandwidth than the Laplace pressure matrix $\mathbf{L}$ in Equation (41). The difference between $\mathbf{L}$ and $\hat{\mathbf{L}}$ provides the necessary stabilization for the accurate solution of Equations (60).

The system of Equations (60) is solved with the following iterative segregated scheme:

Step 1

$$^{j+1}\bar{\mathbf{v}}^{n+1} = \bar{\mathbf{v}}^n + \Delta t \mathbf{M}_d^{-1}[\mathbf{f} - \mathbf{K}^j\bar{\mathbf{v}}^{n+1} - \mathbf{Q}^j\bar{\mathbf{p}}^{n+1}] \tag{61a}$$

Step 2

$$^{j+1}\bar{\mathbf{p}}^{n+1} = [\mathbf{L} - \hat{\mathbf{L}}]^{-1}\mathbf{Q}^{j+1}\bar{\mathbf{v}}^{n+1} \tag{61b}$$

The iterations proceed until a converged solution for $\bar{\mathbf{v}}^{n+1}$ and $\bar{\mathbf{p}}^{n+1}$ is found.

7.1. Differences between the PGPS and the PLS methods

1. In the PGPS method the stabilization parameters are typically taken as constant (at least for homogeneous meshes and constant viscous fluids). In the PLS method, however, the stabilization parameters vary as a function of the volumetric strain rate and the residual of the momentum equations.
2. In the PGPS method the amount of stabilization is varied in space. This variation is introduced by the difference between the Laplace pressure matrix $\mathbf{L}$ and the discrete pressure Laplace matrix $\hat{\mathbf{L}}$. In the PLS method the amount of stabilization is also variable in space, but the variation is introduced by the consistent stabilization parameters τ_i and τ_{b_i}.
3. The consistency in the PGPS method is guaranteed by introducing the discrete residual of the momentum equations $r_{m_i} := (\partial p/\partial x_i) + (1/\hat{\tau}_i)\pi_i$ (no sum in i) in the stabilized mass balance equation (Equation (55)). This term vanishes for the exact solution giving $r_{m_i} = 0$. In the PLS method the consistency is guaranteed by the expression of the stabilization parameters τ_i and τ_{b_i} which also vanish for the exact solution (i.e. for $\varepsilon_v = 0$ and $r_{m_i} = 0$).
4. Both methods are non-linear from the stabilization point of view. The PLS method is non-linear due to the fact that the stabilization parameters are a function of the volumetric strain

DOI: 10.1002/nme

rate, the pressure gradient and the residual of the momentum equations. PGPS methods are non-linear due to the definition of the pressure gradient projection field π_i which is a function of the pressure field.

5. The PLS method introduces a boundary stabilization term which is a function of a constant stabilization parameter multiplied by the volumetric strain rate, which ensures the consistency of the term. The boundary stabilization term is relevant for free surface flow problems.
6. In PSPS methods the boundary stabilization term is usually neglected. This simplification is acceptable on external boundaries because the difference between the pressure gradient and the continuous pressure gradient projection is in general small, but cannot be neglected at internal interfaces with a jump in the physical properties.
7. The PLS method is *a priori* more efficient than the PGPS method as:

   (i) It does not need the evaluation of an auxiliary vector field (i.e. the pressure gradient projections π_i).
   (ii) The bandwidth of the assembled equation system for the pressure is smaller due to the larger bandwidth of the discrete Laplace matrix $\hat{\mathbf{L}}$.
   (iii) As a consequence of (i) and (ii) the computational cost of the PLS method is considerably smaller.
   (iv) The PLS method can represent exactly a pressure gradient jump (Section 9.2).

   The numerical results obtained so far show that the PLS is not only more efficient than the PGPS but in many cases is even more accurate.

8. RELATIONSHIP WITH THE GLS METHOD

The well-known GLS formulation [4, 8] can be readily derived as a particular case of the higher-order FIC formulation presented.

The starting point is the weak form of the higher-order FIC mass balance equations (Equation (16)). From Equation (22) we deduce

$$\frac{\partial \varepsilon_v}{\partial x_i} = \frac{3}{2\mu} r_{m_i} \tag{62}$$

Substituting Equation (62) into (16) gives

$$\int_\Omega q\varepsilon_v \,\mathrm{d}\Omega - \int_\Omega \left(\sum_{i=1}^{2} \tau_i \frac{\partial q}{\partial x_i} r_{m_i} \right) \mathrm{d}\Omega + \int_\Gamma \left(\sum_{i=1}^{2} \tau_i n_i r_{m_i} \right) \mathrm{d}\Gamma = 0 \tag{63}$$

with

$$\tau_i = \frac{h_i^2}{16\mu} \tag{64}$$

It is interesting that this expression for τ_i was obtained in Equation (32) as a particular case of the general form (30).

Note the coincidence of Equation (63) with the enhanced GLS formulation for Stokes flows (including a boundary integral term) presented in [8].

The FIC technique therefore emerges as a 'parent' methodology for deriving a family of stabilized FEM for incompressible continua. A study of the possibilities of the FIC-FEM procedure for these types of problems is presented in [40].

9. EXAMPLES

We have chosen three relative simple, but demonstrative, examples to verify the efficiency and accuracy of the new PLS formulation versus the PGPS method described in Section 7.

DOI: 10.1002/nme

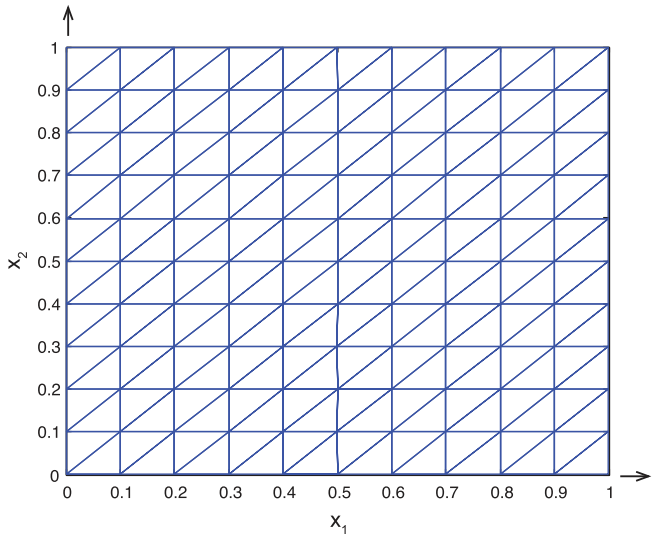

Figure 1. Square analysis domain (1×1 mts) and finite element mesh used.

All the problems studied have been solved in a square container of dimensions 1×1 m using a coarse finite element mesh of $10 \times 10 \times 2$ three-noded triangles (Figure 1). Note that the mesh *is non-symmetrical*. The values of the characteristic distances h_i and h for this problem have been taken simply as $h_1 = h_2 = h = 0.1$ m.

For the PLS method we have used the iterative monolithic scheme of Equation (42a) with the stabilization parameters τ_i defined by Equation (30). For the PGPS method we have used the iterative segregated scheme of Equations (61).

The boundary terms in the stabilized mass balance equation (19) for the PLS method have been found to be irrelevant for the problems solved here.

The solution for $\bar{\mathbf{v}}$ and $\bar{\mathbf{p}}$ has been found in time, starting from a known initial solution with $\bar{\mathbf{v}}^0 = \bar{\mathbf{p}}^0 = \mathbf{0}$. The iterations stop when the increment of the velocity increment vector (in L_2 norm) between two iterations is less than 10^{-10}.

For the first iteration and the first time step, the following initial value of the stabilization parameters has been chosen *for the PLS method*

$$ {}^0\tau_i^1 = {}^0\hat{\tau}^1 = \left[\frac{1}{\dfrac{\rho}{\Delta t} + \dfrac{8\mu}{3l^2}} \right] \quad \text{with } l = 0.1\,\text{m} \tag{65} $$

The above expression coincides with that for the (constant) stabilization parameters for the PGPS method chosen for solving the examples presented next (see Equation (52)).

9.1. *Square water container*

We solve for the pressure distribution in a square container filled with water. The body forces are $b_1 = 0$ and $b_2 = \rho g$ with values of the density and gravity constant equal to $\rho = 1000\,\text{Kg/m}^3$ and $g = -10\,\text{m/s}^2$, respectively. The viscosity is $\mu = 10^{-3}\,\text{Ns/m}^2$. A time increment of $\Delta t = 10^{-2}$ s has been chosen when solving Equation (42a). The normal velocity has been prescribed to zero at the bottom line and the two vertical walls. The nodes on the top surface are allowed to move freely. The solution for this simple problem for the first time step is $\mathbf{v} = \mathbf{0}$ and an hydrostatic distribution of the pressure which is independent of the fluid viscosity. This solution basically does not change in time (except for very small oscillations of the velocity and the pressure).

Figure 2 shows the pressure distribution along the central vertical line obtained with the PLS method for the first time step and different iterations. A converged solution that approximates

DOI: 10.1002/nme

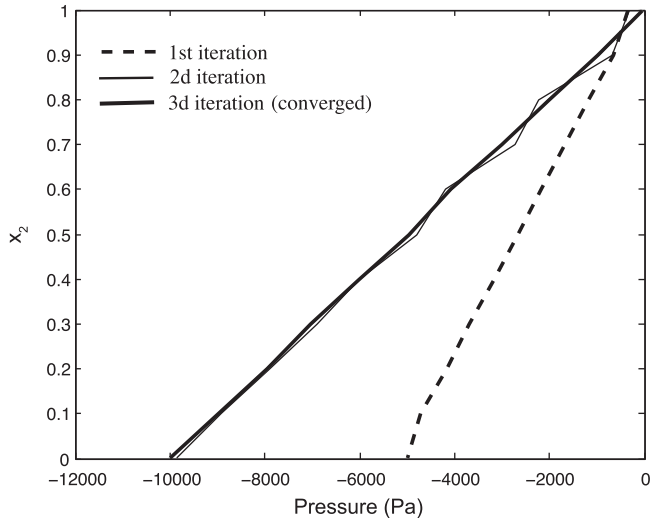

Figure 2. Square container filled with water. Pressure distribution along the central vertical line ($x_1 = 0.5$) obtained with the PLS method.

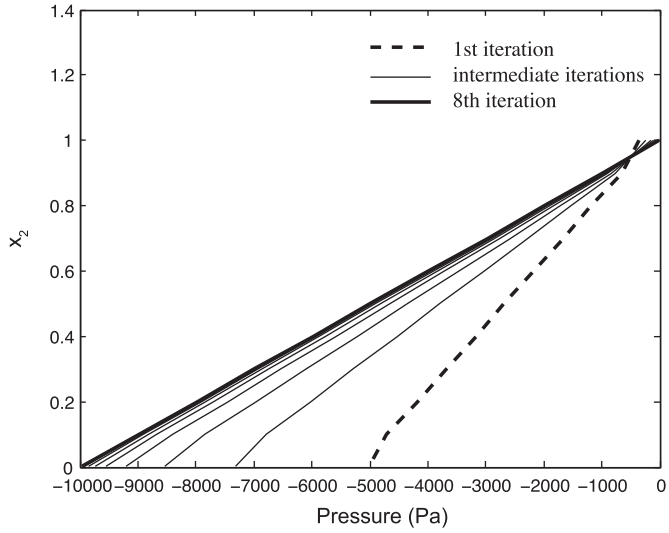

Figure 3. Square container filled with water. Pressure distribution along the central vertical line ($x_1 = 0.5$) obtained with the PGPS method.

practically exactly the hydrostatic distribution is found in *just two iterations*. The same solution is found using the PGPS method *in 8 iterations* (Figure 3).

Figure 4 shows the time evolution of the relative increment of volume in the domain obtained with the PLS method. Note the oscillatory distribution of $\Delta V / V$ with values not exceeding 2.5×10^{-5}. This evidences the good performance of the PLS method in terms of volume preservation.

9.2. Square liquid container with two fluids of different density

The same square container of the previous example is considered assuming that the upper half is filled with a liquid of density $\rho = 10^{-3}\,\mathrm{Kg/m^3}$. The value of the gravity constant is again $g = -10\,\mathrm{m/s^2}$ and the viscosity is the same for both fluids with $\mu = 10^{-3}\,\mathrm{Ns/m^{-2}}$. A time step of $\Delta t = 10^{-3}\,\mathrm{s}$ has been taken. The boundary conditions are the same as for the previous example. The exact analytical solution for the first time step is $\mathbf{v} = 0$ in the whole container and a linear

DOI: 10.1002/nme

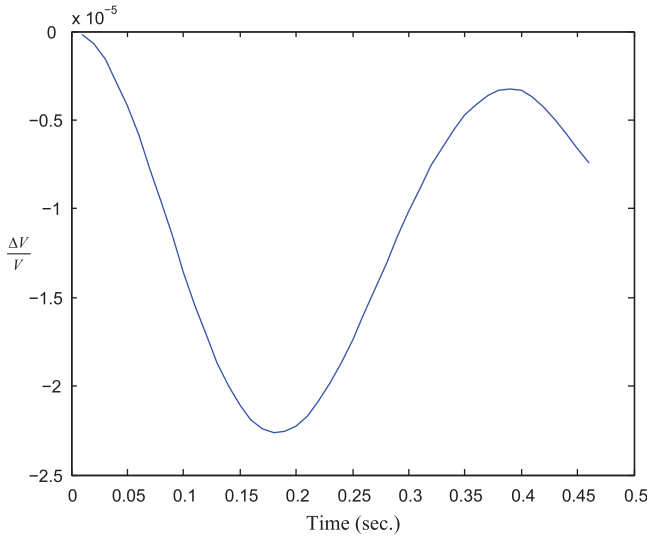

Figure 4. Square container filled with water. Time evolution of the relative volume increment in the domain ($V = 1\,\mathrm{m}^2$). PLS results.

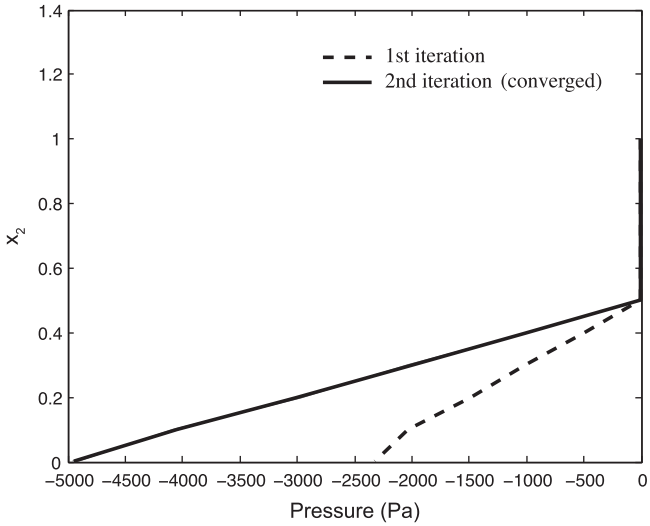

Figure 5. Square container filled with two fluids of different denstiy. Pressure distribution along the central vertical line ($x_1 = 0.5$) obtained with the PLS method.

distribution of the pressure ranging from $p = 0$ at the top ($x_2 = 1.0m$) to $p = 10^{-2}\,\mathrm{Pa}$ at $x_2 = 0.5\,\mathrm{m}$; and again a linear distribution of the pressure from $p = 10^{-2}\,\mathrm{Pa}$ at $x_2 = 0.5\,\mathrm{m}$ to $p = 5,000\,\mathrm{Pa}$ at $x_2 = 0$.

The converged solution for the PLS method is obtained in *just two iterations* (Figure 5). The same solution is found using the PGPS method *in 8 iterations* (Figure 6).

9.3. Driven cavity flow

The flow in a driven square cavity of $1 \times 1\,\mathrm{m}$ is studied the PLS and PGPS methods.

The horizontal velocity on the top surface nodes has been prescribed to $v_1^p(x_1, 1) = 1\,\mathrm{m/s}$. The vertical velocity has also been prescribed to zero at all nodes on the top surface with the exception of the central node with coordinate (0.5,1) which is left free to move in the vertical direction.

DOI: 10.1002/nme

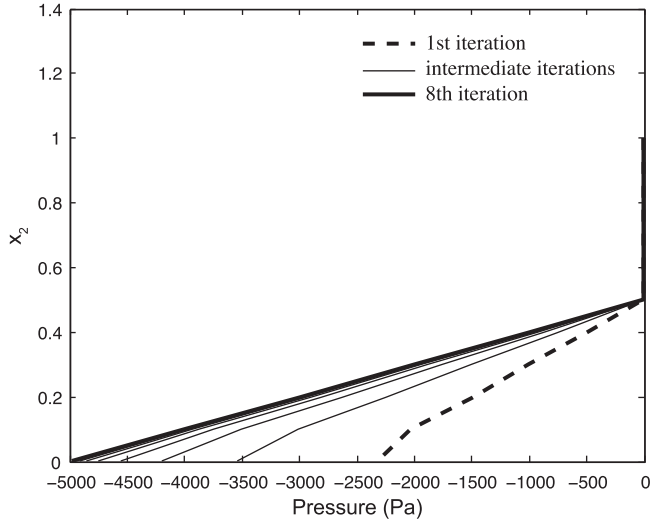

Figure 6. Square container filled with two fluids of different density. Pressure distribution along the central vertical line ($x_1 = 0.5$) obtained with the PGPS method.

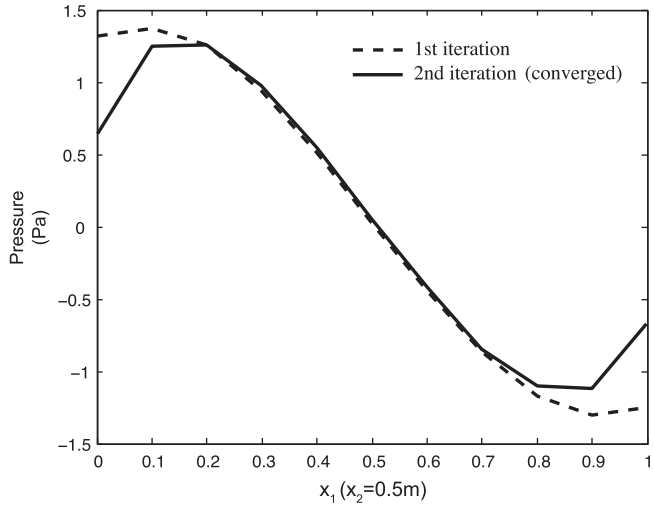

Figure 7. Driven cavity flow. Pressure distribution along the horizontal line for $x_2 = 0.5\,\mathrm{m}$. PLS results.

The normal velocity at the bottom line and the two vertical walls have been prescribed to zero. The physical properties are $\rho = 10^{-10}\,\mathrm{Kg/m^3}$, $g = 0\,\mathrm{N/m^2}$, $\mu = 1\,\mathrm{Ns/m^2}$. The time increment is $\Delta t = 10^{-2}\,\mathrm{s}$.

It can be easily verified that, for the material properties chosen and the values of the pressure and the volumetric strain rate, the value of the stabilization parameter τ_i for the PLS method is approximately constant over the whole analysis domain and equal to

$$\tau_i = \tau \simeq \frac{h_i^2}{16\mu} = \frac{10^{-2}}{16} = 6.25 \times 10^{-3} \frac{\mathrm{m^2 s}}{\mathrm{Kg}} \tag{66}$$

Figure 7 shows the initial solution for the pressure distribution along the horizontal axis for $x_2 = 0.5\,\mathrm{m}$ and the solution found in the second iteration. This solution does not change in an appreciable manner in subsequent iterations. Figure 8 shows the solutions obtained with the PGPS method. The converged solution after eight iterations agrees reasonably well with that found with the PLS method *in just two iterations*.

DOI: 10.1002/nme

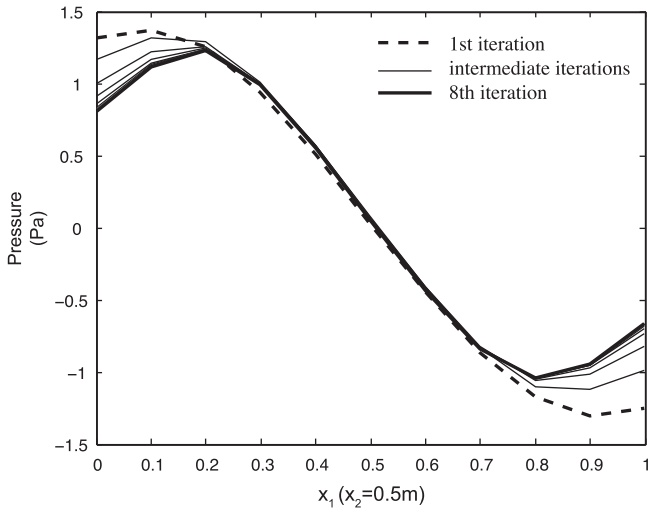

Figure 8. Driven cavity flow. Pressure distribution along the horizontal line for $x_2 = 0.5\,\text{m}$. PGPS results.

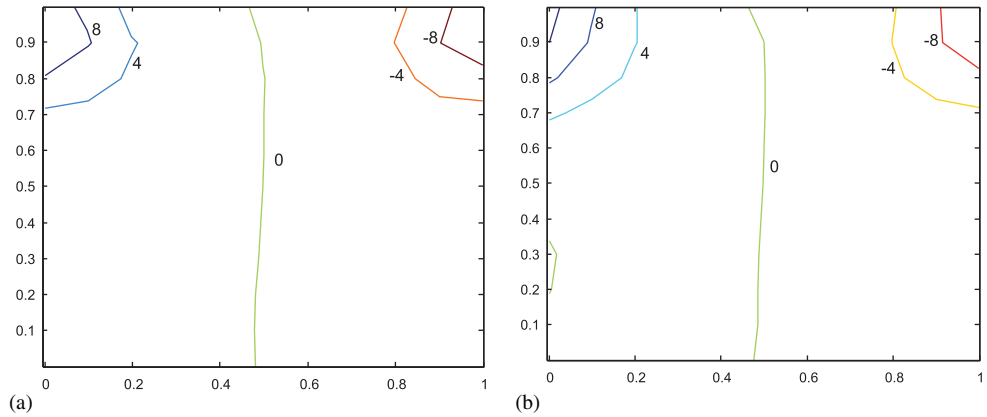

Figure 9. Driven cavity flow. Pressure contours. Numbers indicate the pressure value for the isobar line. (a) PLS method and (b) PGPS method.

A 'correct' solution could have been obtained with the PLS method in just *one iteration* by using the constant value of the stabilization parameter of Equation (66).

Figure 9 shows the pressure contours for both the PLS and PGPS method for the converged solution. Both results are equally good and evidence the singularity of the pressure at the top upper corners. We emphasize again the good results obtained with the PLS method with a coarse *non-symmetric mesh* of three-noded linear triangles.

Similar good results have been obtained for all the problems presented in the paper using four-noded quadrilateral elements with a 2×2 quadrature [40]. In addition, the formulation is directly applicable to non-structured meshes.

For the problems studied the cost of the numerical solutions obtained with the PLS method is considerably less (about one half) that for the PGPS method. More detailed cost studies should be however performed for larger size problems using structured and non-structured meshes.

10. CONCLUDING REMARKS

We have derived a stabilized finite element formulation for incompressible continua via a higher-order FIC method. The method differs from alternative stabilized formulation in that the stabilization

DOI: 10.1002/nme

is introduced in the mass balance equation by a domain pressure Laplacian matrix and a boundary mass matrix multiplied by stabilization parameters, which depend on the discrete residual of the momentum and incompressibility equations. Despite the non-linearity of the stabilized mass balance equation, the convergence to the correct incompressible solution has been found in 2–3 iterations for all the problems studied in the paper.

The PLS method has distinct advantages over alternative stabilization procedures, the main ones being the possibility to operate with just velocity and pressure variables only, the consistent form of the stabilization terms, the natural definition of the stabilization parameters, the preservation of mass for free surface flow problems, the possibility to accurately reproduce pressure gradient jumps in fluids with different densities, the simplicity and reduced bandwith of all the stabilization matrices involved and the fast convergence of the method.

The price to be paid for these advantages is the non-linearity of the stabilized formulation. This might prove to be not so disadvantageous for transient problems (for which the stabilization parameters can be made constant within each time step) or for intrinsically non-linear flows such as Navier-Stokes and non-Newtonian fluid problems.

The good features of the PLS method versus other existing finite element stabilized methods will be verified in more complex flow problems in subsequent work [40].

APPENDIX A

A.1 Derivation of second order FIC mass balance equation

Let us consider the balance of mass in a rectangular domain of dimensions $h_1 \times h_2$ (Figure A1). For simplicity, we denote the horizontal and vertical velocities u and v, respectively. We express the horizontal and vertical velocities at points 1–8 in terms of the values at the center point O. For instance, the horizontal velocities at points 1,2,3 are expressed in terms of the values at the center point using a Taylor series expansion up to third-order terms as follows:

$$u_1 = u_0 + \frac{h_1}{2}u'_{,1} - \frac{h_2}{2}u'_{,2} + \frac{1}{2}\left(\frac{h_1^2}{4}u''_{,1} - \frac{h_1 h_2}{2}u''_{,12} + \frac{h_2^2}{2}u''_{,2}\right)$$

$$+\frac{1}{6}\left[\frac{h_1^3}{8}u'''_{,1} - \frac{3}{8}h_1^2 h_2 u'''_{,112} + \frac{3}{8}h_1 h_2^2 u'''_{,122} - \frac{h_2^3}{8}u'''_{,1}\right] \tag{A1}$$

$$u_2 = u_0 + \frac{h_1}{2}u'_{,1} + \frac{h_1^2}{8}u''_{,1} + \frac{h_1^3}{48}u'''_{,1} \tag{A2}$$

$$u_3 = u_0 + \frac{h_1}{2}u'_{,1} + \frac{h_2}{2}u'_{,2} + \frac{1}{2}\left(\frac{h_1^2}{4}u''_{,1} + \frac{h_1 h_2}{2}u''_{,12} + \frac{h_2^2}{4}u''_{,2}\right)$$

$$+\frac{1}{6}\left(\frac{h_1^3}{8}u'''_{,1} + \frac{3}{8}h_1^2 h_2 u'''_{,112} + \frac{3}{8}h_1 h_2^2 u'''_{,122} + \frac{h_2^3}{8}u'''_{,1}\right) \tag{A3}$$

where

$$(\cdot)'_{,i} = \frac{\partial u}{\partial x_i}, \quad (\cdot)'_{,ij} = \frac{\partial^2 u}{\partial x_i \partial x_j}, \quad (\cdot)'_{,iij} = \frac{\partial^3 u}{\partial x_i \partial x_i \partial x_j}$$

and all the derivatives are computed at the center point 0 with coordinates (x, y).

DOI: 10.1002/nme

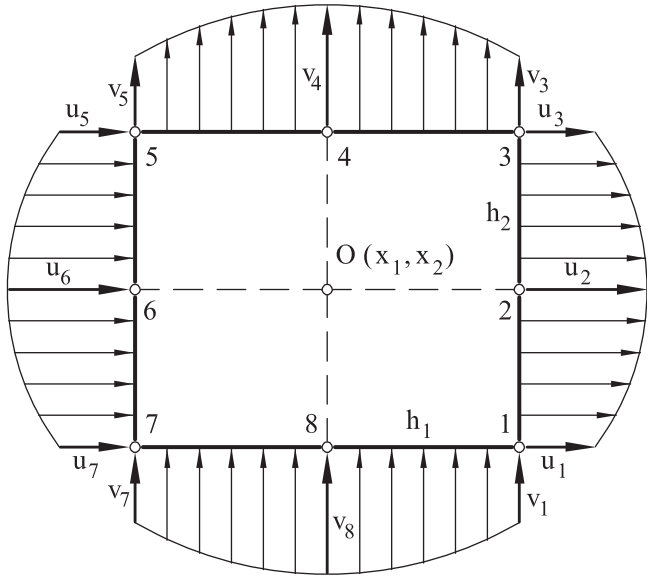

Figure A1. Rectangular mass balance domain $h_1 \times h_2$ in the interior of the body. Parabolic distribution of the velocity along the sides.

Similarly, for points 5,6,7

$$u_5 = u_0 - \frac{h_1}{2}u'_{,1} + \frac{h_2}{2}u'_{,2} + \frac{1}{2}\left(\frac{h_1^2}{4}u''_{,1} - \frac{h_1 h_2}{2}u''_{,12} + \frac{h_2^2}{2}u''_{,2}\right)$$
$$+\frac{1}{6}\left(-\frac{h_1^3}{8}u'''_{,1} + \frac{3}{8}h_1^2 h_2 u'''_{,112} - \frac{3}{8}h_1 h_2^2 u'''_{,122} + \frac{h_2^3}{8}u'''_{,1}\right) \tag{A4}$$

$$u_6 = u_0 - \frac{h_1}{2}u'_{,1} + \frac{h_1^2}{8}u''_{,1} - \frac{h_1^3}{48}u'''_{,1} \tag{A5}$$

$$u_7 = u_0 - \frac{h_1}{2}u'_{,1} - \frac{h_2}{2}u'_{,2} + \frac{1}{2}\left(\frac{h_1^2}{4}u''_{,1} + \frac{h_1 h_2}{2}u''_{,12} + \frac{h_2^2}{4}u''_{,12}\right)$$
$$-\frac{1}{6}\left(\frac{h_1^3}{8}u'''_{,1} + \frac{3}{8}h_1^2 h_2 u'''_{,112} + \frac{3}{8}h_1 h_2^2 u'''_{,122} + \frac{h_2^3}{8}u'''_{,2}\right) \tag{A6}$$

Assuming a parabolic distribution of the horizontal velocity along each edge the balance of mass in the x_1 direction is computed as:

$$\sum \rho u = \rho\frac{h_2}{6}[u_5 + 4u_6 + u_7] - \rho\frac{h_2}{6}[u_1 + 4u_2 + u_3] = -\rho h_1 h_2\left[u'_1 + \frac{1}{24}(h_1^2 u'''_1 + h_2^2 u'''_{,122})\right] \tag{A7}$$

Following an identical procedure the balance of mass in the vertical direction x_2 is obtained as:

$$\sum \rho u = -\rho h_1 h_2\left[v'_{,2} + \frac{1}{24}(h_1^2 v'''_{,122} + h_2^2 v'''_{,2})\right] \tag{A8}$$

The balance of mass in the domain is finally expressed as:

$$\sum \rho(u+v) = -\rho h_1 h_2\left[u'_{,1} + v'_{,2} + \frac{1}{24}h_1^2(u'_{,1} + v'_{,2})''_1 + \frac{1}{24}h_2^2(u'_{,1} + v'_{,2})''_2\right] = 0 \tag{A9}$$

DOI: 10.1002/nme

The higher-order FIC mass balance equation is therefore (defining $u \equiv v_1$ and $v \equiv v_2$)

$$\frac{\partial v_1}{\partial x_1}+\frac{\partial v_2}{\partial x_2}+\frac{h_1^2}{24}\frac{\partial^2}{\partial x_1^2}\left(\frac{\partial v_1}{\partial x_1}+\frac{\partial v_2}{\partial x_2}\right)+\frac{h_2^2}{24}\frac{\partial^2}{\partial x_2^2}\left(\frac{\partial v_1}{\partial x_1}+\frac{\partial v_2}{\partial x_2}\right)=0 \tag{A10}$$

or

$$\boxed{\varepsilon_v+\frac{h_1^2}{24}\frac{\partial^2 \varepsilon_v}{\partial x_1^2}+\frac{h_2^2}{24}\frac{\partial^2 \varepsilon_v}{\partial x_2^2}=0} \quad \text{in } \Omega \tag{A11}$$

with

$$\varepsilon_v=\frac{\partial v_1}{\partial x_1}+\frac{\partial v_2}{\partial x_2}=\frac{\partial v_i}{\partial x_i} \tag{A12}$$

Clearly for the infinitesimal case $h_1=h_2=0$ and the standard form of the mass balance equation ($\varepsilon_v=0$) is recovered.

APPENDIX B

We will derive first the expressions for the stabilization parameters given in Equation (33).

From Equations (24) and (25) the following identities hold:

$$\frac{2}{3}\mu|\nabla\varepsilon_v|=|\mathbf{r}_m| \tag{B1}$$

$$\frac{\rho|h_\xi|}{2}|\mathbf{v}||\nabla\varepsilon_v|=\rho|\mathbf{v}||\varepsilon_v| \tag{B2}$$

$$\rho\frac{h_\xi^2}{4\Delta t}|\nabla\varepsilon_v|=\frac{\rho|h_\xi|}{2\Delta t}|\varepsilon_v| \tag{B3}$$

From Equations (B1)–(B3) we deduce

$$|\nabla\varepsilon_v|=\frac{\left(\rho|\mathbf{v}|+\dfrac{\rho|h_\xi|}{2\Delta t}\right)|\varepsilon_v|+|\mathbf{r}_m|}{\dfrac{\rho|h_\xi\mathbf{v}|}{2}+\rho\dfrac{h_\xi^2}{4\Delta t}+\frac{2}{3}\mu} \tag{B4}$$

Substituting Equation (B4) into Equation (18) gives

$$\tau_i=\frac{h_i^2}{|\nabla p|}\frac{\left(\rho|\mathbf{v}|+\dfrac{\rho|h_\xi|}{2\Delta t}\right)|\varepsilon_v|+|\mathbf{r}_m|}{\left(12\rho|h_\xi\mathbf{v}|+6\rho\dfrac{h_\xi^2}{\Delta t}+16\mu\right)} \tag{B5}$$

which is the sought expression for τ_i.

For the derivation of the expression for τ_i of Equation (34) we proceed as follows. From Equations (10), (11) and (24) we deduce the following identities:

$$\rho|h_\xi\mathbf{v}|\frac{|\nabla p|}{|\nabla\varepsilon_v|}=\rho|h_\xi\mathbf{v}|\left|\frac{p}{\varepsilon_v}\right| \tag{B6}$$

$$\mu\frac{|\nabla p|}{|\nabla\varepsilon_v|}=\frac{2}{3}\mu^2\frac{|\nabla p|}{|\mathbf{r}_m|} \tag{B7}$$

DOI: 10.1002/nme

Combining Equations (B6) and (B7) gives

$$\frac{|\nabla p|}{|\nabla \varepsilon_v|} = \frac{\rho |h_\xi \mathbf{v}| \left| \dfrac{p}{\varepsilon_v} \right| + \frac{2}{3}\mu^2 \dfrac{|\nabla p|}{|\mathbf{r}_m|}}{\rho |h_\xi \mathbf{v}| + \mu} \tag{B8}$$

Substituting Equation (B8) into Equation (18) gives

$$\tau_i = h_i^2 \left[\frac{\rho |h_\xi \mathbf{v}| + \mu}{24\rho |h_\xi \mathbf{v}| |\frac{p}{\varepsilon_v}| + 16\mu^2 \dfrac{|\nabla p|}{|\mathbf{r}_m|}} \right] \tag{B9}$$

which is the sought expression for τ_i.

ACKNOWLEDGEMENTS

The authors thank Drs J. García, R. Rossi and Messrs P. Nadukandi and M.A. Celigueta for many useful discussions. Support for this research was provided by the SEDUREC project of the Consolider Programme of the Ministry of Science and Innovation of Spain and from the REALTIME project of the European Research Council of the European Commission. This work was also supported by Publishing Arts Research Council under grant 98-1846389.

The work of the third author was partly supported through a Visiting Professor fellowship awarded by the Spanish Ministerio de Educación y Cultura.

REFERENCES

1. Donea J, Huerta A. *Finite Element Method for Flow Problems*. Wiley: 2003.
2. Zienkiewicz OC, Taylor RL, Nietharasu P. The finite element method. *Fluid Mechanics*, vol. 3. Elsevier: Amsterdam, 2005.
3. Brooks AN, Hughes TJR. Streamline upwind Petrov–Galerkin formulation for convective dominated flows with particular emphasis on the incompressible Navier–Stokes equations. *Computer Methods in Applied Mechanics and Engineering* 1982; **32**:199–259.
4. Hughes TJR, Franca LP, Balestra M. A new finite element formulation for computational fluid dynamics. V. Circumventing the Babuska–Brezzi condition: A stable Petrov–Galerkin formulation of the Stokes problem accomodating equal order interpolations. *Computer Methods in Applied Mechanics and Engineering* 1986; **59**:85–99.
5. Franca LP, Frey SL. Stabilized finite element methods: II. The incompressible Navier–Stokes equations. *Computer Methods in Applied Mechanics and Engineering* 1992; **99**:209–233.
6. Hughes TJR, Hauke G, Jansen K. Stabilized finite element methods in fluids: inspirations, origins, status and recent developments. In *Recent Developments in Finite Element Analysis* A Book Dedicated to, Taylor RL, Hughes TJR, Oñate E, Zienkiewicz OC (eds). International Center for Numerical Methods in Engineering (CIMNE): Barcelona, Spain, 1994; 272–292.
7. Tezduyar TE, Mittal S, Ray SE, Shih R. Incompressible flow computations with stabilized bilinear and linear equal order interpolation velocity–pressure elements. *Computer Methods in Applied Mechanics and Engineering* 1992; **95**:221–242.
8. Droux J-J, Hughes TJR. A boundary integral modification of the Galerkin least squares formulation for the Stokes problem. *Computer Methods in Applied Mechanics and Engineering* 1994; **113**:173–182.
9. Storti M, Nigro N, Idelsohn SR. Steady state incompressible flows using explicit schemes with an optimal local preconditioning. *Computer Methods in Applied Mechanics and Engineering* 1995; **124**:231–252.
10. Cruchaga MA, Oñate E. A finite element formulation for incompressible flow problems using a generalized streamline operator. *Computer Methods in Applied Mechanics and Engineering* 1997; **143**:49–67.
11. Codina R, Vazquez M, Zienkiewicz OC. A general algorithm for compressible and incompressible flow—part III. The semi-implicit form. *International Journal for Numerical Methods in Fluids* 1998; **27**:13–32.
12. Cruchaga MA, Oñate E. A generalized streamline finite element approach for the analysis of incompressible flow problems including moving surfaces. *Computer Methods in Applied Mechanics and Engineering* 1999; **173**:241–255.
13. Tezduyar TE, Osawa Y. Finite element stabilization parameters computed from element matrices and vectors. *Computer Methods in Applied Mechanics and Engineering* 2000; **190**:411–430.
14. Hughes TJR, Mazzei L, Jansen KE. Large eddy simulation and the variational multiscale method. *Computing and Visualization in Science* 2000; **3**:47–59.

DOI: 10.1002/nme

15. Codina R. Stabilization of incompressibility and convection through orthogonal sub-scales in finite element methods. *Computer Methods in Applied Mechanics and Engineering* 2000; **190**:1579–1599.
16. Codina R, Blasco J. A finite element formulation for the Stokes problem allowing equal velocity–pressure interpolation. *Computer Methods in Applied Mechanics and Engineering* 2000; **143**:373–391.
17. Codina R, Blasco J. Stabilized finite element method for the transient Navier–Stokes equations based on a pressure gradient operator. *Computer Methods in Applied Mechanics and Engineering* 2000; **182**:277–301.
18. Codina R, Zienkiewicz OC. CBS versus GLS stabilization of the incompressible Navier-Stokes equations and the role of the time step as stabilization parameter. *Communications Numerical Methods in Engineering* 2002; **18**(2):99–112.
19. Dohrmann CR, Bochev PB. A stabilized finite element method for the stokes problem based on polynomial pressure projections. *International Journal for Numerical Methods in Fluids* 2004; **46**:183–201.
20. Codina R, Principe J, Guasch O, Badia S. Time dependent subscales in the stabilized finite element approximation of incompressiblity flow problems. *Communications in Numerical Methods in Engineering* 2007; **196**(2):2413–2430.
21. Badia S, Codina R. On a multiscale approach to the transient Stokes problem. Transient subscales and anistropic space–time discretization. *Applied Mathematics and Computation* 2009; **207**:415–433.
22. Oñate E. Derivation of stabilized equations for advective–diffusive transport and fluid flow problems. *Computer Methods in Applied Mechanics and Engineering* 1998; **151**:233–267.
23. Oñate E. A stabilized finite element method for incompressible viscous flows using a finite increment calculus formulation. *Computer Methods in Applied Mechanics and Engineering* 2000; **182**(1–2):355–370.
24. Oñate E, García J. A finite element method for fluid–structure interaction with surface waves using a finite calculus formulation. *Computer Methods in Applied Mechanics and Engineering* 2001; **191**:635–660.
25. Oñate E, Taylor RL, Zienkiewicz OC, Rojek J. A residual correction method based on finite calculus. *Engineering Computations* 2003; **20**(5/6):629–658.
26. Oñate E. Possibilities of finite calculus in computational mechanics. *International Journal for Numerical Methods in Engineering* 2004; **60**(1):255–281.
27. Oñate E, Idelsohn SR, Del Pin F, Aubry R. The particle finite element method. An overview. *International Journal of Computational Methods* 2004; **1**(2):267–307.
28. Idelsohn SR, Oñate E, Del Pin F. The particle finite element method: a powerful tool to solve incompressible flows with free-surfaces and breaking waves. *International Journal for Numerical Methods in Engineering* 2004; **61**:964–989.
29. Oñate E, Rojek J, Taylor RL Zienkiewicz OC. Finite calculus formulation for incompressible solids using linear triangles and tetrahedra. *International Journal for Numerical Methods in Engineering* 2004; **59**:1473–1500.
30. Oñate E, Valls A, García J. FIC/FEM formulation with matrix stabilizing terms for incompressible flows at low and high Reynolds numbers. *Computational Mechanics* 2006; **38**(4–5):440–455.
31. Oñate E, García J, Idelsohn SR, Del Pin F. FIC formulations for finite element analysis of incompressible flows. Eulerian, ALE and Lagrangian approaches. *Computer Methods in Applied Mechanics and Engineering* 2006; **195**(23–24):3001–3037.
32. Oñate E, Valls A, García J. Modeling incompressible flows at low and high Reynolds numbers via a finite calculus-finite element approach. *Journal of Computational Physics* 2007; **224**:332–351.
33. Oñate E, Idelsohn SR, Celigueta MA, Rossi R. Advances in the particle finite element method for the analysis of fluid–multibody interaction and bed erosion in free surface flows. *Computer Methods in Applied Mechanics and Engineering* 2008; **197**(19–20):1777–1800.
34. Idelsohn SR, Mier-Torrecilla M, Oñate E. Multi-fluid flows with the particle finite element method. *Computer Methods in Applied Mechanics and Engineering* 2009; **198**:2750–2767.
35. Idelsohn SR, Del Pin F, Rossi R, Oñate E. Fluid–structure interaction problems with strong added-mass effect. *International Journal for Numerical Methods in Engineering* 2009; **80**(10):1261–1294.
36. Zienkiewicz OC, Taylor RL. *The Finite Element Method for Solid and Structural Mechanics*, vol. 2. Butterworth-Heinemann: London, 2005.
37. Idelsohn SR, Marti J, Limache A, Oñate E. Unified Lagrangian formulation for elastic solids and incompressible fluids: application to fluid-structure interaction problems via the PFEM. *Computer Methods in Applied Mechanics and Engineering* 2008; **197**:1762–1776.
38. de Mier Torrecilla M. Numerical simulation of multi-fluid flows with the particle finite element method. *Ph.D. Thesis*, Technical University of Catalonia (UPC), July 2010.
39. Idelsohn SR, Oñate E. The challenge of mass conservation in the solution of free-surface flows with the fractional-step method: problems and solutions. *Communications in Numerical Methods in Engineering* 2008; DOI: 10.1002/cnm.1216.
40. Oñate E, Nadukandi P, Idelsohn SR, García J, Felippa C. A family of residual-based stabilized finite element methods for Stokes flows. *Research Repot IT-599*, CIMNE, Barcelona, July 2010. Submitted to International Journal for Numerical Methods in Fluids.
41. Idelsohn SR, Mier-Torrecilla M, Nigro N, Oñate E. On the analysis of heterogeneous fluids with jumps in the viscosity using a discontinuous pressure field. *Computational Mechanics* 2010; **46**(1):115–124.